

Stabilisation of the Arrival Time of a High Energy Electron Beam at the 50 fs Level

J. Roberts,^{1,2,*} P. Burrows,¹ G. Christian,¹ R. Corsini,² A. Ghigo,³ F. Marcellini,³ C. Perry,¹ and P. Skowronski²

¹*John Adams Institute, University of Oxford*

²*CERN, Geneva*

³*INFN/LNF, Frascati*

(Dated: February 27, 2017)

CLIC, a proposed future linear electron-positron collider, and other machines such as XFELs, place tight tolerances on the phase stabilities of their beams. CLIC proposes the use of a novel, high bandwidth and low latency, ‘phase feedforward’ system required to achieve a phase stability of 0.2° at 12 GHz, or about 50 fs. This work documents the results from operation of a prototype phase feedforward system at the CLIC test facility CTF3, with 30 MHz bandwidth and a total hardware latency of 100 ns. New phase monitors with 30 fs resolution, 20 kW amplifiers with 47 MHz bandwidth, and electromagnetic kickers have been designed and installed for the system. The system utilises a dog-leg chicane in the beamline, for which a dedicated optics have been created and commissioned. The prototype has demonstrated CLIC-level phase stability, reducing an initial rms phase variation of $0.92 \pm 0.04^\circ$ to $0.20 \pm 0.01^\circ$ across a duration of 10 minutes.

INTRODUCTION

The Compat Linear Collider, CLIC, [1] is a proposal for a future linear electron-positron collider. It uses a novel two beam acceleration concept to achieve a high accelerating gradient of 100 MV/m and a collision energy of up to 3 TeV. In this concept the 12 GHz RF power used to accelerate each high energy colliding beam is extracted and transferred from a high intensity drive beam in 24 decelerator sectors. **The drive beams are generated by compressing an initial 140 μ s beam pulse bunched at 0.5 GHz into 24 shorter 240 ns beam pulses bunched at 12 GHz using a sequence of so-called combiner rings and delay loops [REF].**

CLIC’s luminosity quickly drops if the RF phase jitters with respect to the main beam, causing energy errors and subsequent beam size growth at the interaction point. The RF phase stability must be 0.2° at 12 GHz (around 50 fs) rms or better to limit the luminosity loss to below 1% [1]. However, the phase, or arrival time, stability of the RF producing drive beam pulses cannot be guaranteed to be better than 2° at 12 GHz. A mechanism to improve the drive beam phase stability by an order of magnitude is therefore required.

Other machines, such as XFELs, have similar beam phase stability requirements to CLIC. At FLASH, DESY, these requirements have been met using an RF phase and power feedback based on the measurement of electro-optic beam arrival time monitors [REF]. However, the CLIC drive beam presents a different set of challenges. In particular, FLASH has 1 MHz bunch spacing and a 500 ms beam pulse, whereas the CLIC drive beam has 12 GHz bunch spacing and 240 ns pulse length. A feedback with a latency of several microseconds is therefore not suitable for CLIC.

CLIC instead proposes a drive beam “phase feedforward” (PFF) system.

Some details on CLIC system

The PFF system poses many challenges, particularly in terms of the hardware bandwidth (>17.5 MHz [2]), power (500 kW amplifiers) and latency requirements. A prototype PFF system has therefore been designed, commissioned and operated at the CLIC test facility CTF3, at CERN, to prove its feasibility. The prototype system follows the same concept as the proposed CLIC scheme, and is the focus of this work.

CTF3 provides a 135 MeV electron beam bunched at 3 GHz with a pulse length of 1.2 μ s and a pulse repetition rate of 0.8 Hz [REF]. All phases quoted in the paper are given in degrees at 12 GHz.

SYSTEM DESIGN

A schematic of the PFF system is shown in Fig. 1. The system corrects the phase using two electromagnetic kickers installed before the first and last dipole in a four bend chicane (in the TL2 transfer line). The beam’s path length through the chicane depends on the magnitude and polarity of the voltage applied to the kickers. The phase is measured using a monitor upstream of the chicane (in the CT beam line), and then corrected by setting the kicker voltage to deflect bunches arriving early at the phase monitor on to longer trajectories in the chicane, and bunches arriving late on to shorter trajectories. Downstream of the chicane, in the TBL line, another phase monitor is placed to measure the effects of the correction.

The beam time of flight between the upstream phase monitor and the first kicker in the chicane is 380 ns. By bypassing the combiner ring (CR) and TL1 transfer line (see Fig. 1) the total cable length required to transport signals between the monitor and kickers is shorter, approximately 250 ns. The PFF correction in the chicane can therefore be applied to the same bunch initially measured at the phase monitor, providing the total system

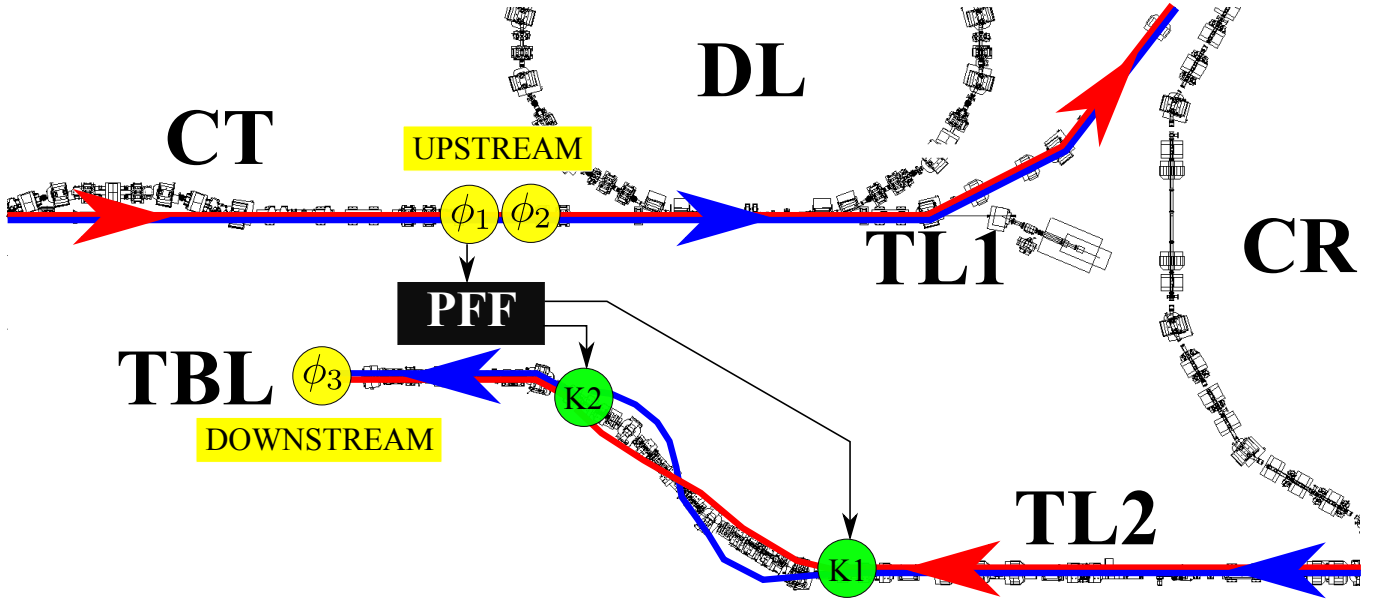


FIG. 1. Schematic of the PFF prototype at CTF3, showing the approximate location of the phase monitors (ϕ_1 , ϕ_2 and ϕ_3) and the kickers (K1 and K2). The black box PFF represents the calculation and output of the correction, including the phase monitor electronics, feedforward controller and kicker amplifiers. A bunch arriving early at ϕ_1 is directed on to a longer path in the TL2 chicane using the kickers (blue trajectory), whereas a bunch arriving late will be directed on to a shorter path (red trajectory).

hardware latency is less than 130 ns.

Hardware

The PFF system uses three phase monitors, two electromagnetic kickers, kicker amplifiers and a digitiser/feedforward controller.

The three phase monitors [3] are designed and built by INFN Frascati, with the associated electronics built by CERN. The monitors are 12 GHz resonating cavities with a dipole and monopole mode present. The output from opposing vertical pairs of feedthroughs are summed in hybrids to create a position independent signal. This signal is split and mixed with a reference 12 GHz signal in eight separate mixers. The output from the eight mixers is combined, allowing a resolution of 0.12° to be achieved whilst maintaining linearity between $\pm 70^\circ$ [REF]. The quoted resolution is determined by comparing the measurements of the two adjacent upstream monitors (installed in the CT line, see Fig. 1).

The two electromagnetic stripline kickers [4] were also designed and built by INFN Frascati, and are based on the DAFNE design [REF]. Each kicker is approximately 1 m in length, with a horizontal strip separation of 40 mm. A voltage of 1.26 kV applied to the downstream end of the kicker strips yields a horizontal deflection of 1 mrad for the 135 MeV CTF3 beam.

The kicker amplifiers [5] have been designed and built by the John Adams Institute/Oxford University. The

20 kW amplifiers consist of low voltage Si FETs driving high voltage SiC FETs, and for an input voltage of ± 2 V give an output of up to ± 700 V. The amplifier response is linear within 3% for input voltages between ± 1.2 V, then starts to saturate. The output has a bandwidth of 47 MHz for small signal variations up to 20% max output, and is slew rate limited for larger variations.

Finally, the Feedforward digitiser and controller (FONT5a board) [5] was also designed and built by John Adams Institute/Oxford University. This digitises the processed phase monitor signals and then calculates and outputs the appropriate voltage with which to drive the amplifier in order to correct the phase. The board consists of a Virtex-5 field programmable gate array (FPGA), nine 14-bit analogue to digital converters (ADCs) clocked at 357 MHz, and four digital to analogue converters (DACs). The parameters of the correction, such as the system timing and gain, are controlled on the board via a LabVIEW data acquisition and control system.

The combined hardware latency for the PFF system is approximately 100 ns. The output from the FONT5a board is delayed by 30 ns so that the drive voltage from the amplifiers and the beam arrive at the kickers synchronously.

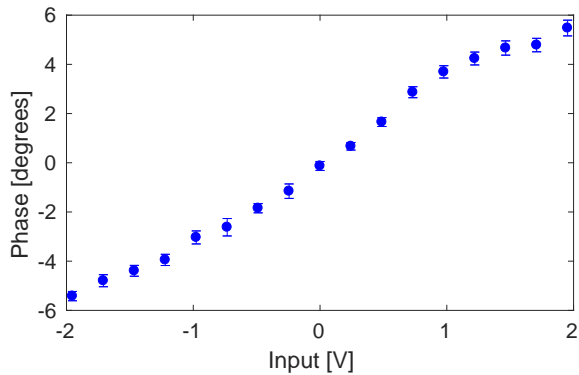


FIG. 2. Downstream phase vs. the kicker amplifier input voltage. Standard errors on the measured phase are shown.

Chicane Optics

The PFF system places additional constraints on the optics of the correction chicane, and also on the beam lines between the upstream phase monitor and the chicane. These ensure the maximum possible phase shift per volt applied to the kickers without degrading the transverse beam orbit and beam size after the chicane, and high correlation between the initial (uncorrected) upstream and downstream phase.

The correction range of the PFF system is defined by the kicker design, the maximum output voltage of the kicker amplifiers, and the optics transfer matrix coefficient R_{52} between the kickers in the chicane, which relates the change in path length through the chicane per unit deflection at the first kicker. For the maximum amplifier output of ± 700 V the kickers deflect the beam by ± 0.56 mrad. Together with $R_{52} = 0.74$ m in the chicane optics these define the system correction range of approximately ± 400 μ m, or $\pm 6^\circ$.

The measured phase shift in the chicane versus the amplifier input voltage is shown in Fig. 2, and agrees with the expected range. However, the response of the amplifier and therefore the phase shift is non-linear. The correction algorithm assumes linearity, but this has a negligible effect compared to the limitations placed by the upstream-downstream phase correlation and phase monitor resolution.

The PFF system also should not change the beam orbit after the chicane. The chicane optics are designed so that the second kicker closes the orbit bump created by the first kicker. Fig. 3 shows the horizontal beam orbit in the region of the chicane for the maximum and minimum kick. The closure in the BPMs following the chicane is better than 0.1 mm, compared to a maximum offset of 1.5 mm inside the chicane.

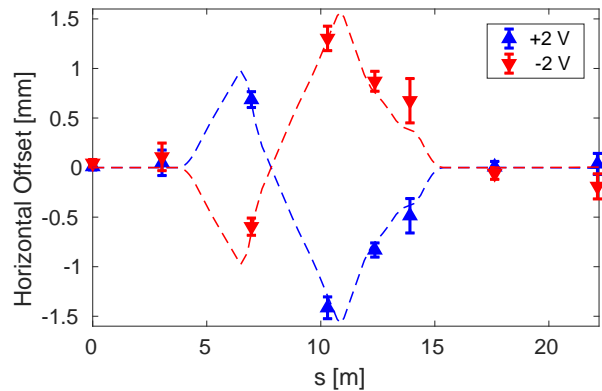


FIG. 3. Horizontal orbit in and around the TL2 chicane at maximum (blue) and minimum (red) input to the kicker amplifiers. Markers show the measured position in beam position monitors, and dashed lines the predicted orbit using the CTF3 MADX model and hardware parameters.

Phase Correlation

The PFF system acts to subtract the measured upstream phase (ϕ_u) from the initial downstream phase (ϕ_d) with a gain factor (g): $\phi_{\text{PFF}} = \phi_d - g\phi_u$, where ϕ_{PFF} is the corrected downstream phase. The optimal system gain is given by: $g = \rho_{ud}\sigma_d/\sigma_u$, where σ_u and σ_d are the initial upstream and downstream phase jitter respectively, and ρ_{ud} is the correlation between the upstream and downstream phase. The theoretical limit on the corrected downstream phase jitter (σ_{PFF}) with this gain is given by: $\sigma_{\text{PFF}} = \sigma_d\sqrt{1 - \rho_{ud}^2}$.

One of the key challenges in operating the PFF prototype at CTF3 has been obtaining high correlation between the initial, uncorrected, upstream and downstream phase. A correlation of 97% is required to reduce a typical initial phase jitter of 0.8° at CTF3 to the target of 0.2° .

The achievable correlation depends on the phase monitor resolution and any additional phase jitter introduced in the beam lines between the upstream and downstream phase monitors. The phase monitor resolution of 0.12° limits the maximum upstream-downstream phase correlation to 98% in typical conditions, and places a theoretical limit of 0.17° on the measured corrected downstream phase jitter.

Any beam jitter that changes the time of flight of bunches influences the resulting downstream phase stability and upstream-downstream phase correlation. The dominant source of uncorrelated downstream phase jitter at CTF3 is beam energy jitter being transformed in to phase jitter in the transfer lines between the upstream and downstream phase monitors.

The first order phase-energy dependence can be described via the optics transfer matrix coefficient R_{56} :

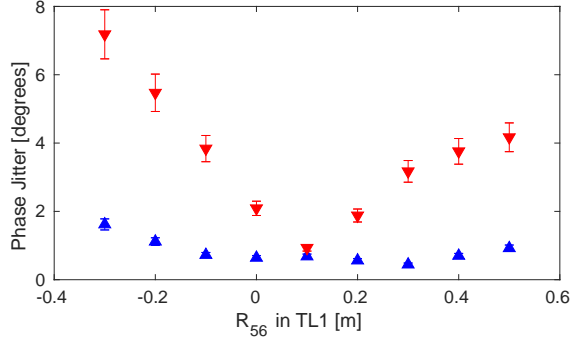


FIG. 4. Downstream (red points) and upstream (blue points) phase jitter vs. the R_{56} value in the set TL1 optics.

$\phi_d = \phi_u + R_{56}(\Delta p/p)$, where $\Delta p/p$ is the relative beam energy offset. Optimal conditions for the PFF system are obtained when the total R_{56} between the upstream and downstream monitors is zero. The R_{56} value in one of the transfer lines at CTF3, TL1, has been tuned in order to achieve this, compensating for R_{56} terms in other beam lines. Fig. 4 shows that with an R_{56} of around 10 cm in TL1 the downstream phase jitter is reduced to the same level as the upstream jitter. The upstream-downstream phase correlation is also increased to above 95%.

However, a large second order phase-energy dependence was also identified and this remains uncorrected. This leads to a degradation in upstream-downstream phase correlation if there are drifts in beam energy. Energy drifts resulting from klystron trips and RF power drifts at CTF3 have made it difficult to maintain high phase correlations for timescales longer than 10 minutes as a result.

RESULTS

Gain Scan

With the optimal gain the PFF correction acts to remove all correlation between the upstream and downstream phase, reducing the downstream phase jitter. If the gain is too small some residual correlation will remain, and if it is too large the correlation will flip sign.

The optimal system gain can be derived empirically by observing the dependence of the downstream phase on the upstream phase with the correction on, as seen in Fig. 5. Optimal gain values for the system are typically in the range 1.0–1.5, being larger than unity when the downstream jitter is larger than upstream, as per the predicted theoretical values.

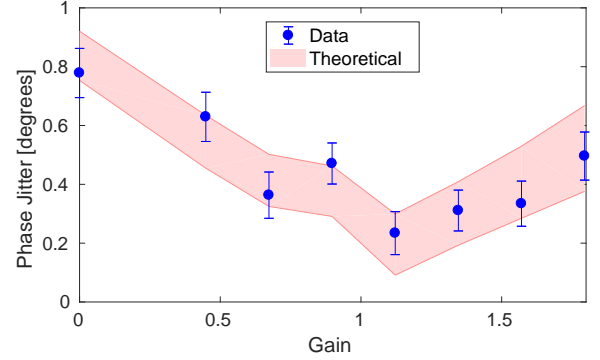


FIG. 5. Downstream phase jitter with the PFF system on at different gains. Markers show the measured phase jitter with standard error bars. The shaded red region shows the expected performance given the initial jitter and correlation with the PFF system off.

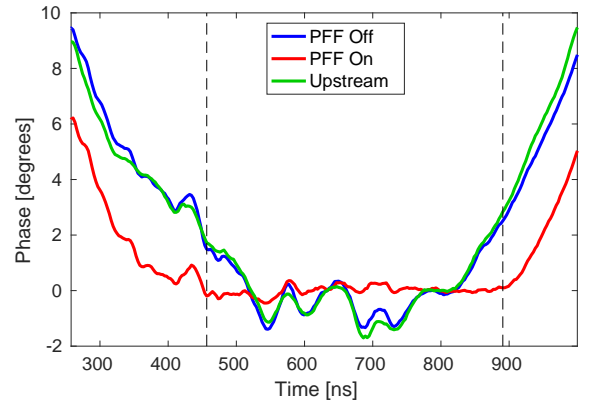


FIG. 6. Effect of the PFF system on intra-pulse phase variations. The pulse shape upstream (green), and downstream with the PFF system off (blue) and on (red) is shown.

Intra-Pulse Phase Variations

The PFF correction is shaped to remove phase variations along the $1.2 \mu\text{s}$ CTF3 beam pulse. The predominant intra-pulse feature at CTF3 is a roughly parabolic “phase sag” of 40° peak-to-peak, resulting from the use of RF pulse compression. As this is much larger than the $\pm 6^\circ$ range of the PFF system, only approximately a 400 ns portion of the pulse can be optimally corrected. The phase sag would not be present at CLIC, where in any case the drive beam pulse length is less than 400 ns.

Fig. 6 shows the effect of the PFF system on the intra-pulse phase variations. **The convention at CTF3 is to operate the PFF system in interleaved mode, with the correction applied to alternating pulses only. This allows a measurement of the initial (‘PFF Off’) and corrected (‘PFF On’) downstream phase to be performed concurrently.** The upstream (PFF input) phase is also shown

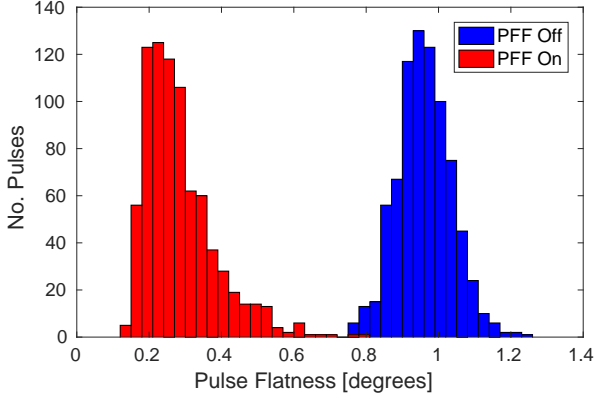


FIG. 7. Distribution of downstream rms phase values, here referred to as the “pulse flatness”, for each beam pulse with the PFF system off (blue) and on (red).

for comparison. Vertical dashed lines mark a 440 ns portion of the pulse where the correction is optimal, and this range is used to calculate statistics on the effect of the system.

In this range the PFF system flattens the phase, and almost all variations are removed. Residual offsets in the phase are still present where there are small uncorrelated differences between the shape of the initial upstream and downstream phase. Fig. 7 shows the rms phase variation within the 440 ns range for each beam pulse in the dataset, with the PFF system on and off. The PFF off pulses have an rms of $0.960 \pm 0.003^\circ$ on average, and this is reduced to $0.285 \pm 0.004^\circ$ by the PFF system.

The PFF system at CTF3 has been verified to reduce the amplitude of phase errors up to a frequency of 25 MHz, exceeding the CLIC requirements.

Pulse-to-pulse Jitter

As well as removing intra-pulse phase variations the PFF system simultaneously corrects offsets in the overall mean phase, i.e. any pulse-to-pulse jitter. The mean phase of each beam pulse is calculated across the 440 ns range in the central portion of the pulse, as shown before in Fig. 6.

Fig. 8 shows the effect of the PFF system on the pulse-to-pulse stability across a dataset around ten minutes in length. An initial mean downstream phase jitter of $0.92 \pm 0.04^\circ$ is reduced to $0.20 \pm 0.01^\circ$ by the PFF correction. All correlation between the upstream and downstream jitter is removed, from $96 \pm 2\%$ to $0 \pm 7\%$. The achieved stability is consistent with the theoretical prediction (considering the initial correlation and jitter) of $0.26 \pm 0.06^\circ$ within error bars.

This level of stability could not be maintained for longer periods due to CTF3’s drifting RF sources, even-

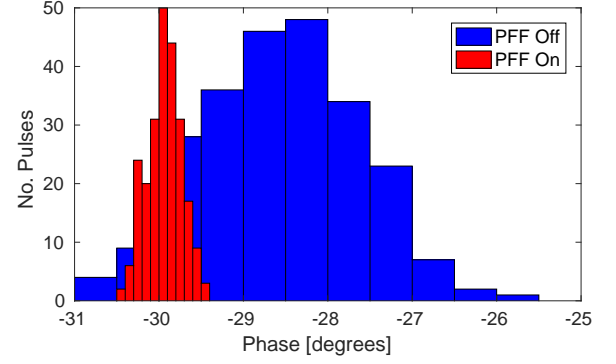


FIG. 8. Distribution of the mean downstream phase with the PFF system off (blue) and on (red).

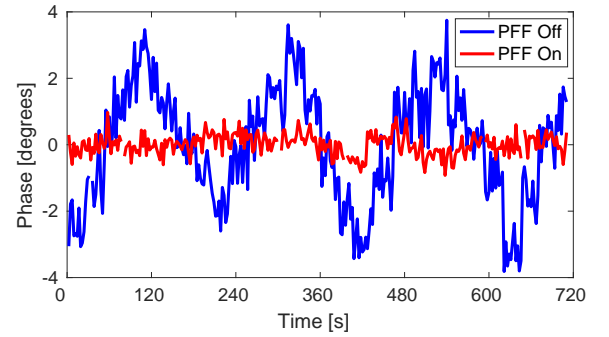


FIG. 9. Mean downstream phase with the PFF system off (blue) and on (red) vs. time, with additional phase variations added to the incoming phase.

tually leading to degraded upstream-downstream phase correlation and phase drifts outside the PFF correction range, as previously mentioned. 0.30° phase jitter has been achieved in 20 minute datasets. With suitable feedbacks to keep the phase within the correction range, and a reduction of the higher order phase-energy dependences in the machine optics, the PFF system could achieve CLIC-level phase stability continuously.

The PFF system has also been operated whilst intentionally varying the incoming mean phase, as shown in Fig. 9. The PFF system removes the additional phase variations and achieves more than a factor 5 reduction in downstream phase jitter, from $1.71 \pm 0.07^\circ$ to $0.32 \pm 0.01^\circ$ in this case.

CONCLUSIONS

CLIC requires a PFF system to reduce the drive beam phase jitter by an order of magnitude, from 2.0° to 0.2° at 12 GHz, or better than 50 fs stability. A prototype of the system has been in operation at the CLIC test facility CTF3, and corrects the beam phase by varying the path length through a chicane using two electromagnetic

kickers.

As well as the kickers, the system uses newly designed phase monitors with 0.12° resolution, high bandwidth 20 kW amplifiers and a low latency digitiser/feedforward controller. The system latency, including hardware and signal transit times, is less than the 380 ns beam time of flight between the input phase monitor and the correction chicane. Therefore, the feedforward correction can be directly applied to the same bunch initially measured at the monitor.

New optics for the correction chicane and other beam lines at CTF3 have been developed to yield the desired phase shifting behaviour and ensure high correlation between the initial upstream and downstream phase.

The prototype system has demonstrated $0.20 \pm 0.01^\circ$ pulse-to-pulse phase jitter on a time scale of ten minutes. It has also been shown to be able to flatten intra-pulse phase variations up to a frequency of 25 MHz. On longer timescales the performance of the system is limited by changes to the incoming beam conditions, in particular beam energy, which would be better controlled in any future application at CLIC.

SOME FIGURES

ACKNOWLEDGEMENTS

We wish to acknowledge everyone involved in the operation of CTF3 for their help and support in realising the PFF system.

* Corresponding author Jack.Roberts@cern.ch

- [1] M. Aicheler *et al.*, “A multi-TeV linear collider based on CLIC technology: CLIC conceptual design report,” CERN-2012-007 (2012).
- [2] A. Gerbershagen *et al.*, Phys. Rev. AB **18**, 041003 (2015).
- [3] F. Marcellini *et al.*, “RF phase monitor final report,” EuCARD-REP-2013-023 (2014).
- [4] A. Ghigo *et al.*, in *Proceedings of IPAC2011*, Vol. TUPC007 (San Sebastian, Spain, 2011) pp. 1000–1002.
- [5] J. Roberts, *Development of a Beam-based Phase Feedforward Demonstration at the CLIC Test Facility (CTF3)*, DPhil thesis, University of Oxford (2016).

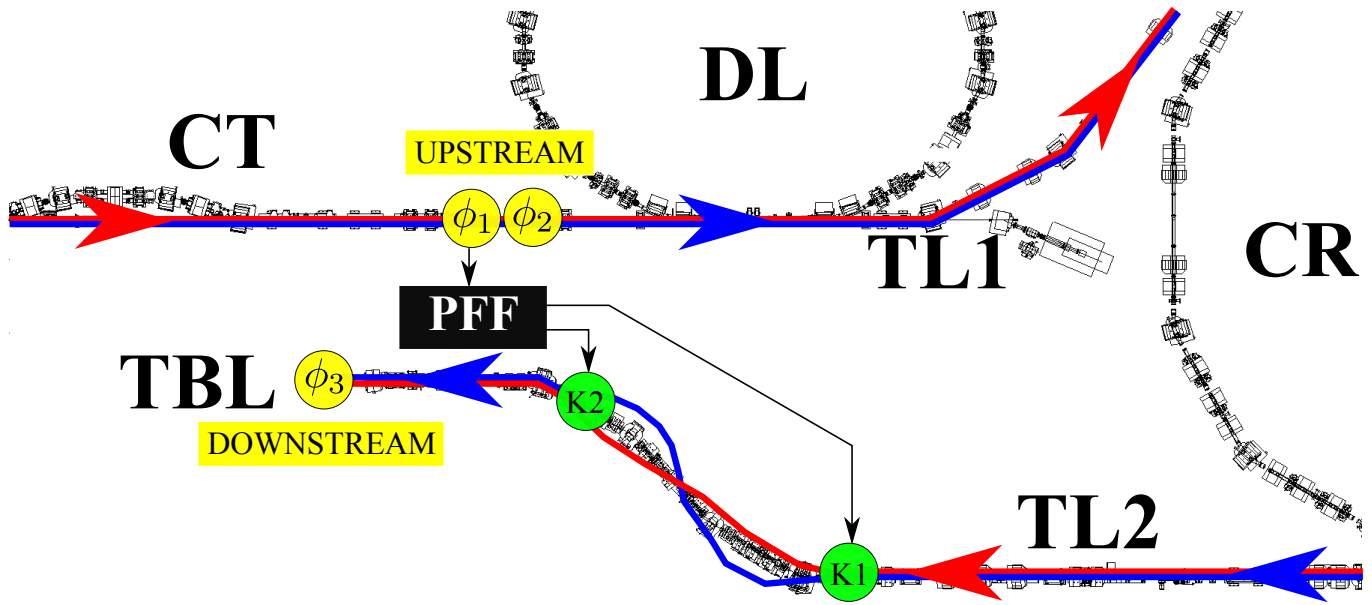


FIG. 10.

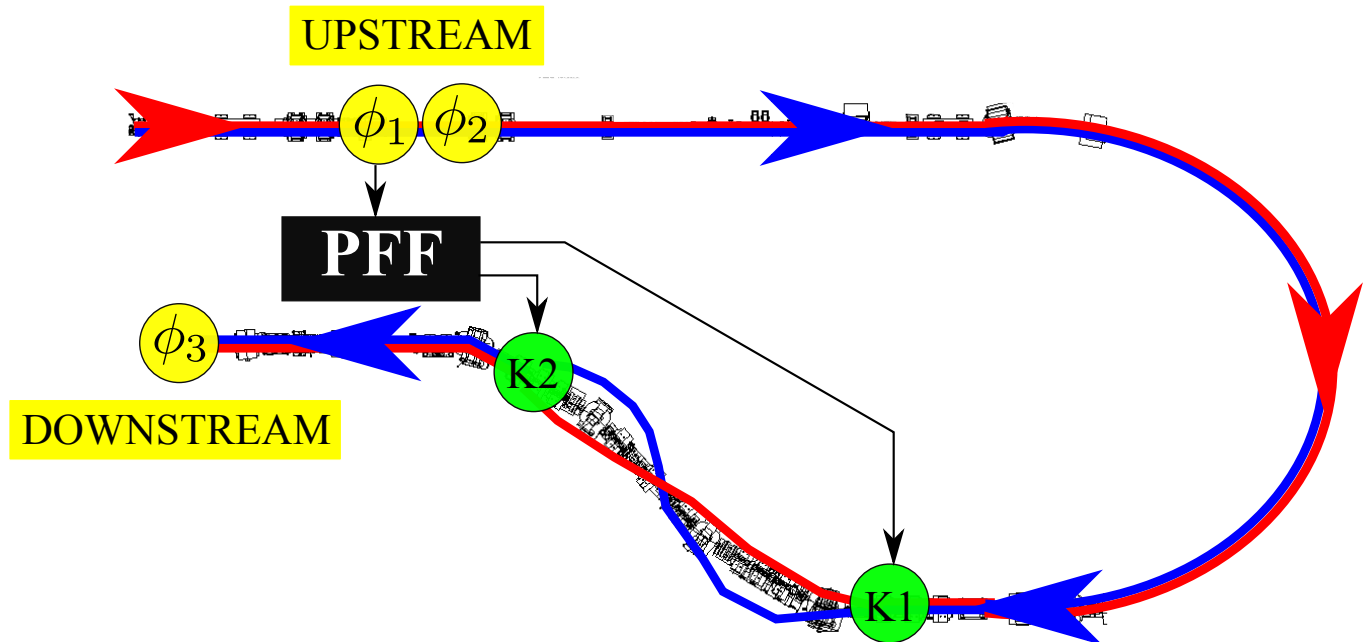


FIG. 11.

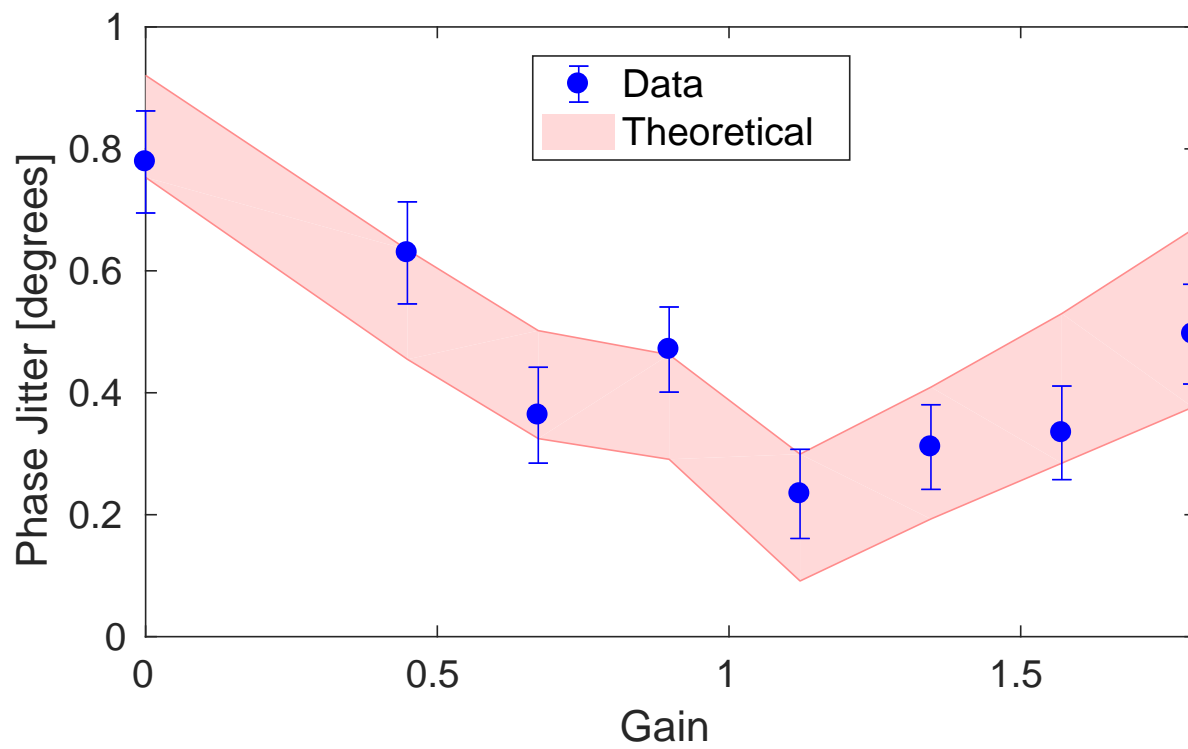


FIG. 12.

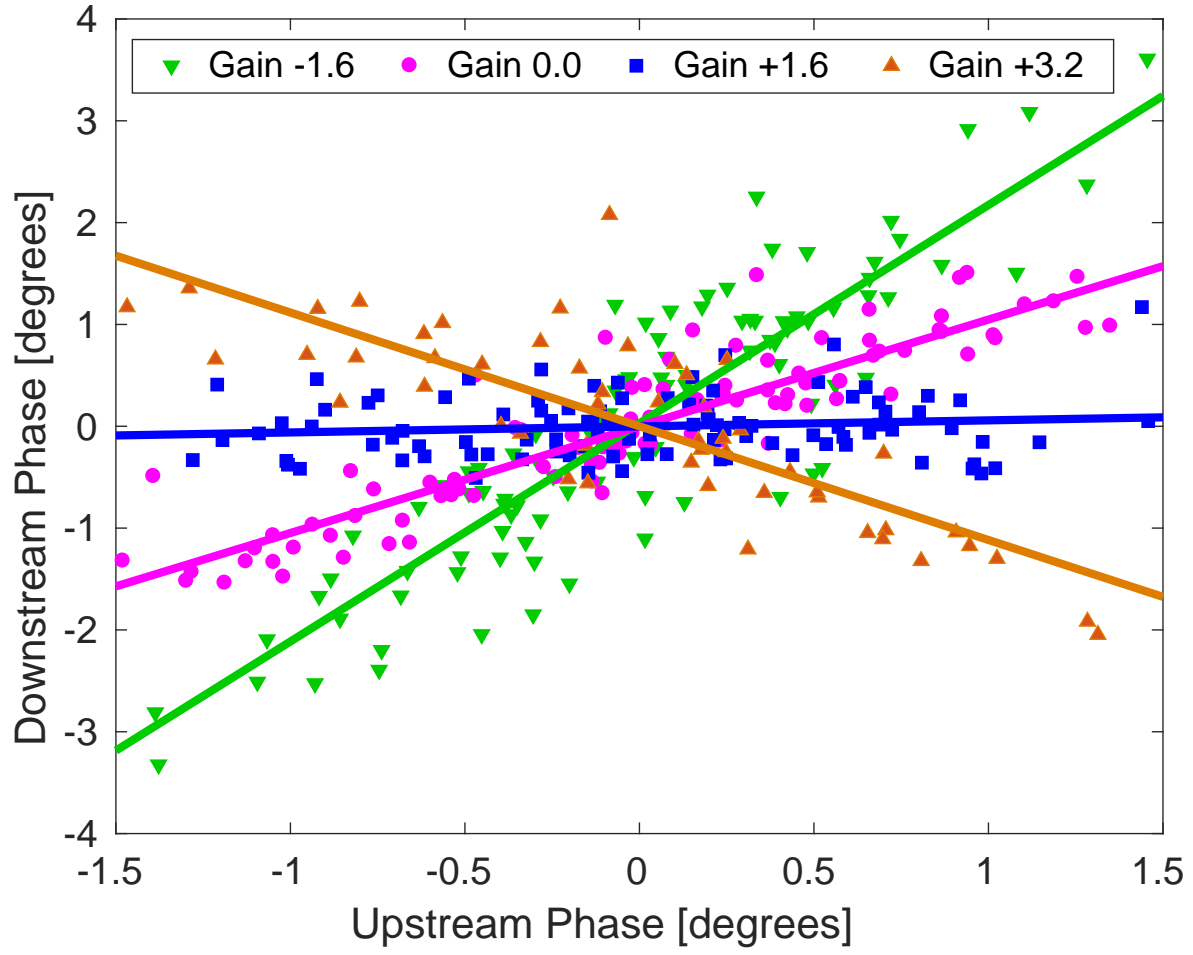


FIG. 13.

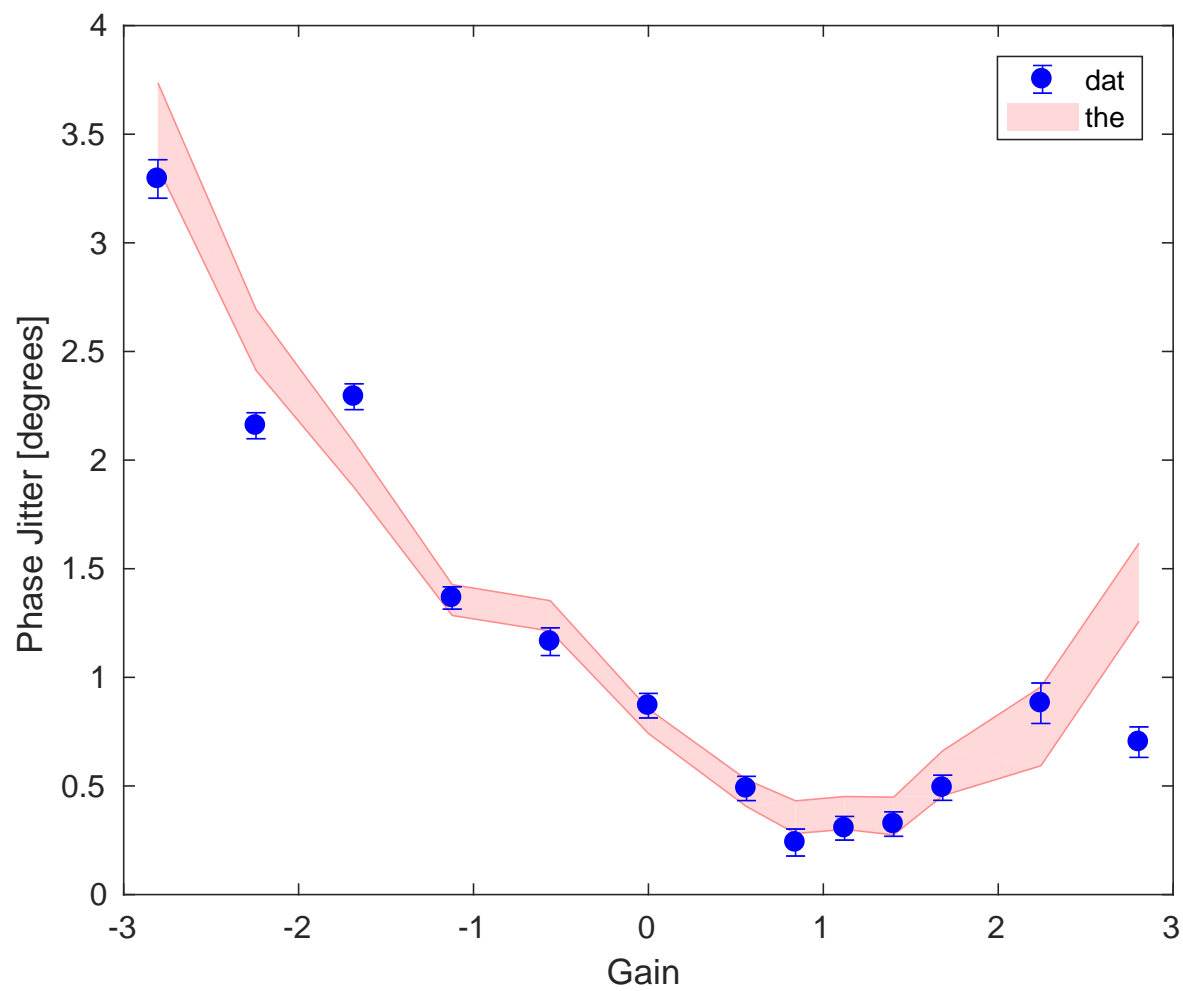


FIG. 14.

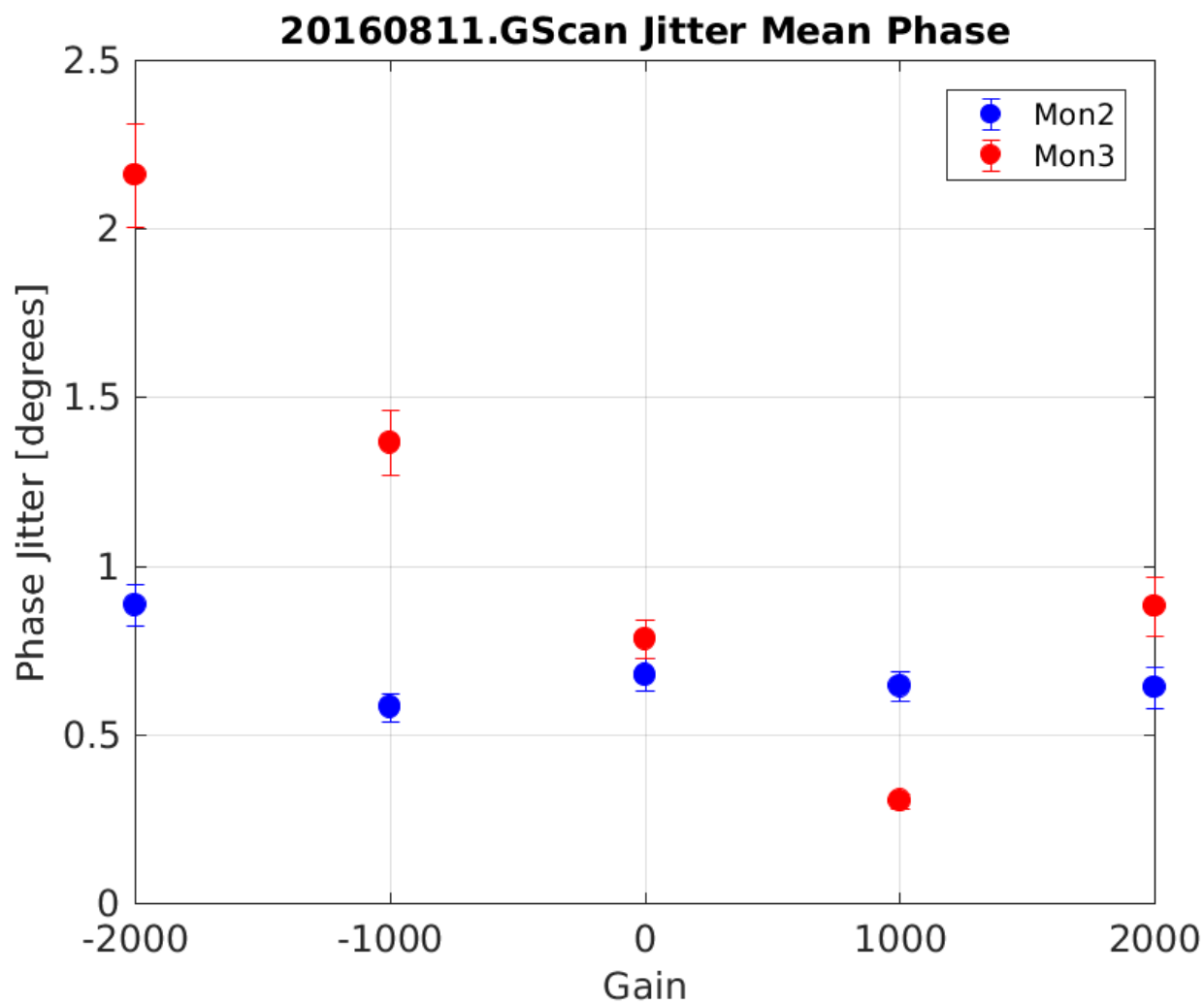


FIG. 15.

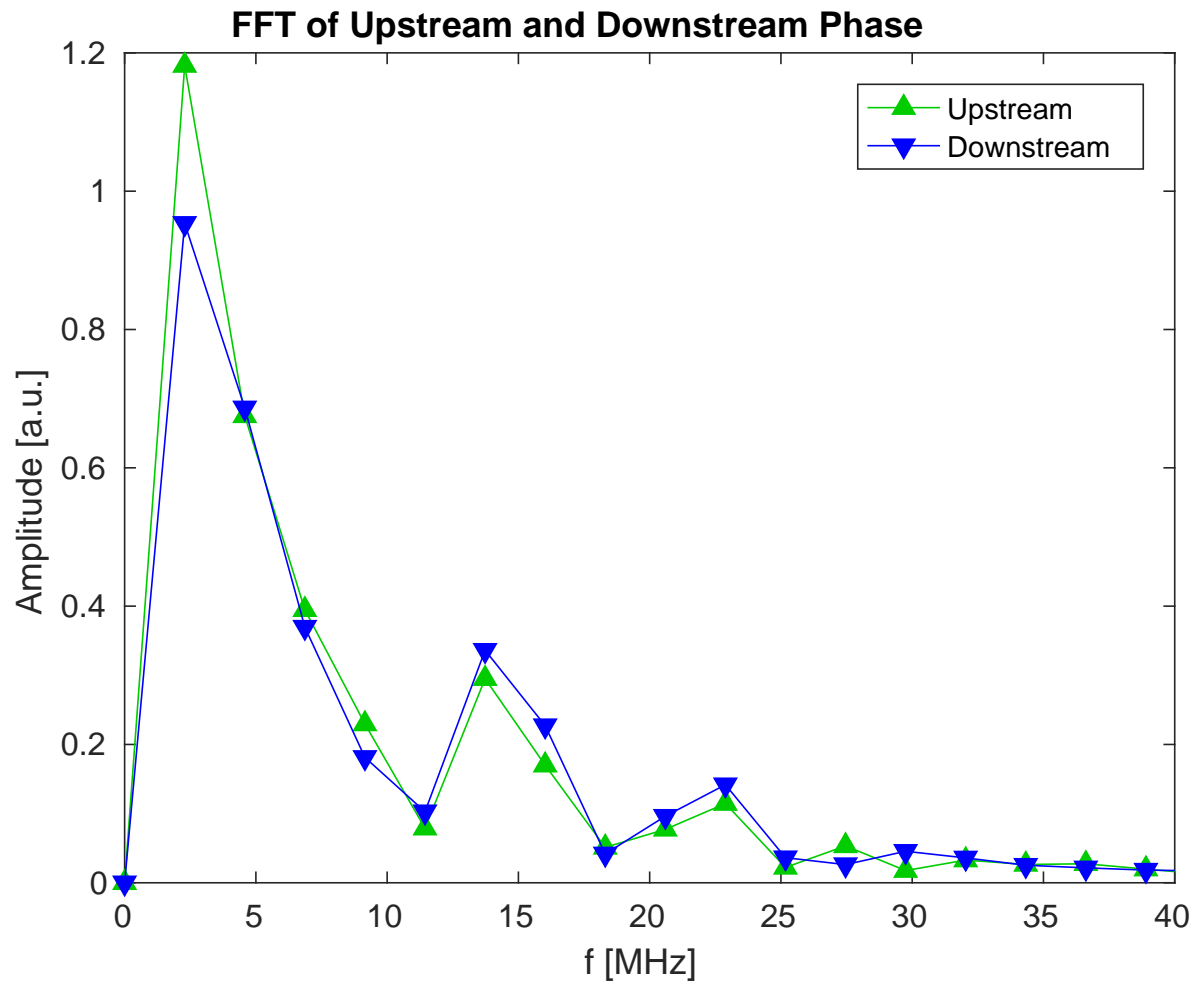


FIG. 16.

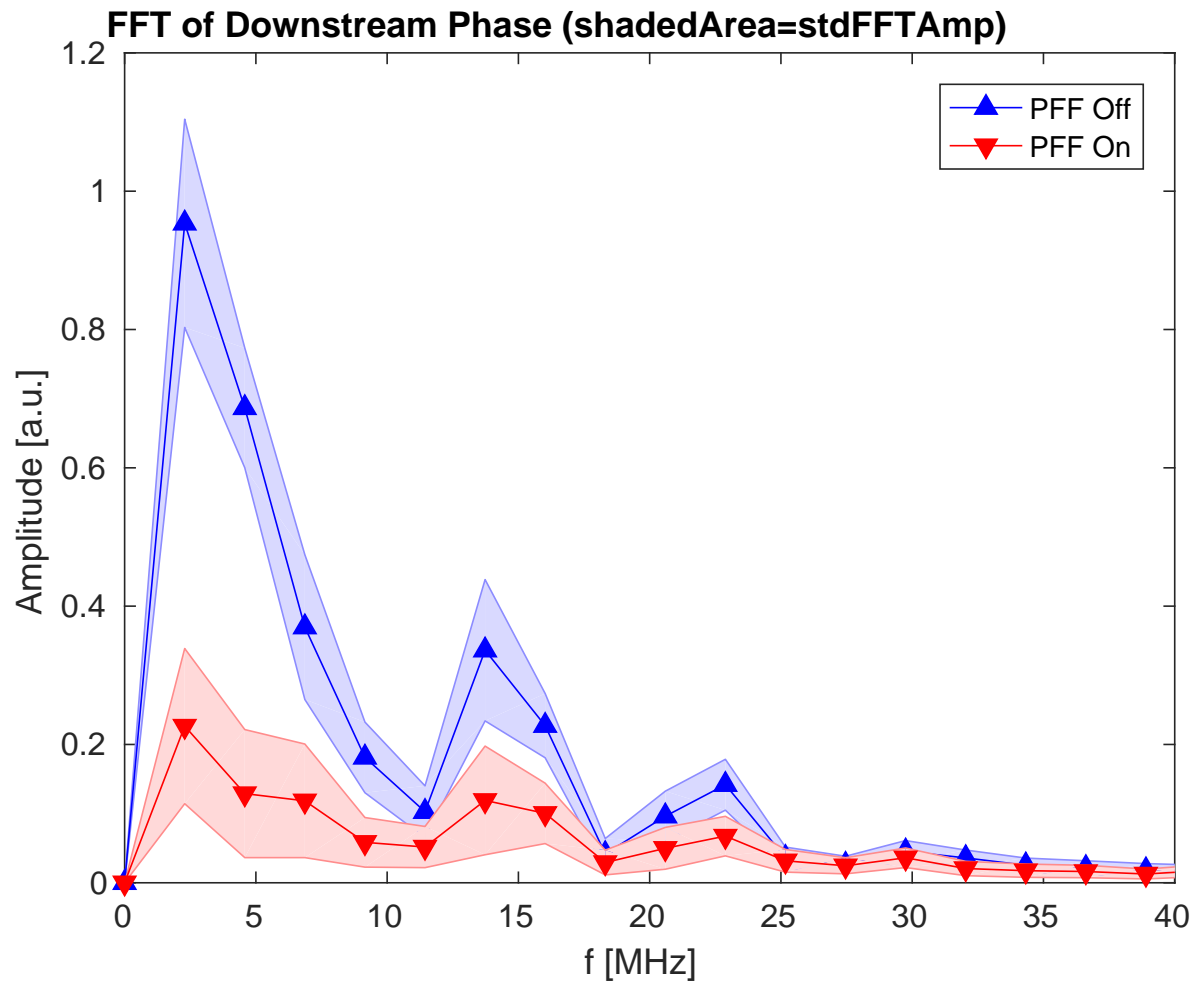


FIG. 17.